Molecular Simulation of Capillary Phenomena in Controlled Pore Glasses

Lev D. Gelb[†] **and K. E. Gubbins**[*]

[†]Florida State University
Department of Chemistry
Tallahassee, FL 32306-4390, USA
(E-mail: gelb@chem.fsu.edu)

[*]North Carolina State University
Department of Chemical Engineering
Raleigh, NC 27695-7905, USA
(E-mail: keg@ncsu.edu)

Abstract

We have developed molecular models for porous glasses that reproduce the complex network structures of these materials. Large-scale simulations of xenon adsorption and desorption isotherms are performed in a series of models with varying network connectivity. The shape of the adsorption/desorption hysteresis loop does *not* appear to depend on the connectivity of the material model, supporting the hypothesis that in materials of this type (e.g., Vycor glass) the fluid in different pores behaves quasi-independently, and that no system-spanning transition occurs during adsorption or desorption.

1. Introduction

Controlled pore glasses and porous Vycor glasses have proven to be convenient and popular systems for the experimental study of capillary condensation [1–4], and are one of the best-characterized porous materials with a non-trivial network structure. Our object in this study is to better understand the effects of this network structure on the adsorptive behavior of these materials, and especially how the connectivity of the material mediates the presence or absence of system-spanning phase transitions. Our approach in this work is to use molecular simulations on a large scale to study adsorption and desorption in qualitatively reasonable models of these materials. Molecular simulation affords a microscopic, pore-by-pore view of adsorption and desorption which is difficult or impossible to develop by other means; furthermore, we exploit the ability to manipulate the microstructure of the models in order to determine the effects of microstructural changes on capillary phenomena.

2. Preparation of Glass Models

The original preparations and characterizations of controlled pore glasses were done by Haller [5]. The starting material is 50–75% SiO_2, 1–10% Na_2O, and the remainder B_2O_3. The molten glass mixture is phase-separated by cooling to between 500 and 750 °C; the time taken for this treatment determines the extent of phase separation and the resulting average pore size. The borate phase is leached out by acid solutions at high temperatures. The remaining glass contains colloidal silica particles, which are removed by a treatment with NaOH followed by washing with water. The final glass has a porosity between 50% and 75%, an average pore size between 4.5 nm and 400 nm, and surface area between 10 and 350 m^2/g [6]. Vycor glasses are prepared by a similar procedure [7]. Vycors have a porosity near 28%, mean pore diameter between 4 and 6 nanometers, and surface area between 90 and 200 m^2/g [7].

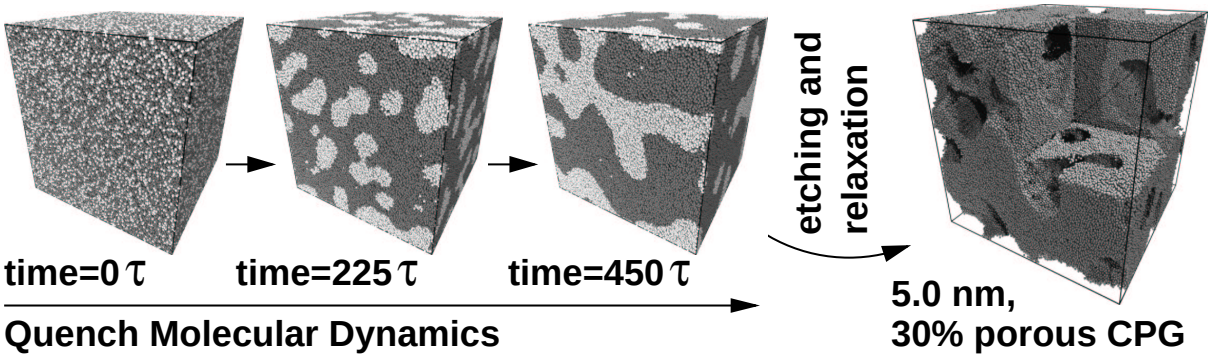

Figure 1. Procedure for the generation of model materials. Quench molecular dynamics simulations of a binary Lennard-Jones mixture produce networked structures via spinodal decomposition, which are then processed into model adsorbents. Quench configurations taken at longer times yield progressively larger-pore materials. Simulation time is given in Lennard-Jones reduced units.

In previous work [8,9] we have developed a procedure for the preparation of models of these materials which mimics the preparation of experimental glasses. These models have reasonable pore sizes, porosities and surface areas, and are similar in appearance. A schematic of this procedure is shown in *Figure 1*.

For the study presented here, the model material was prepared using a simulation cell 27 nm on each side, initially containing 868,000 particles. This model has 30% porosity and 5.0 nm mean pore size, measured geometrically [9]. BJH analysis of simulated nitrogen isotherms gives a value closer to 4.5 nm [9], which is more relevant for comparison with adsorption-characterized experimental materials, despite the known shortcomings of the method [9].

3. GCMC Simulations

Grand Canonical Monte Carlo is a stochastic scheme which simulates an *open* system with fixed temperature, chemical potential, and volume. It is the appropriate method to use for determining adsorption isotherms by computer simulation. The specific details and mathematics of this scheme can be found elsewhere [10].

In order to simulate adsorption of xenon in these model pores, we represent xenon by a Lennard-Jones sphere with potential parameters $\sigma_{\mathrm{Xe}} = 0.391$ nm and $\varepsilon_{\mathrm{Xe}}/k_B = 227$ K. The parameters for the substrate atoms are set to $\sigma = 0.27$ nm and $\varepsilon/k_B = 230$ K, which have been used to represent bridging oxygens in silica [11]. Reduced quantities are given in terms of these units. The Lorenz-Berthelot mixing rules were used for inter-species parameters. Interactions between xenon atoms were truncated at $2.5\sigma_{\mathrm{Xe}}$, while interactions between xenon atoms and pore atoms were cut-and-shifted at the same radius. No long-range corrections were used [10].

The adsorption calculations were performed using a variant of the parallelized GCMC algorithm suggested by Heffelfinger and Lewitt [12]. In this approach, the simulation cell is divided into volumes assigned to each processor. Each of these volumes is then subdivided into eight rectilinear sub-cells. The essence of the algorithm is that, because of the short range of the potential, Monte Carlo moves made in non-adjacent sub-cells can be evaluated independently; no global collection of the total energy or total number of particles is necessary. This requires that the acceptance criteria for creation and destruction moves only involve the sub-cell volume and sub-cell density; appropriate criteria have appeared in the literature [13]. In each cycle, a fixed number of moves are made in one sub-cell by each processor. A round of communication follows in which each processor updates all of its neighbors on its current atomic positions. Each processor then makes a fixed number of moves in the *next* sub-cell, and the process continues, with periodic synchronization and output.

In this study, all isotherm data were obtained using a $3 \times 3 \times 3$ domain decomposition (27 processors) on IBM SP and Cray T3E computers. Points at low pressure and at pressures

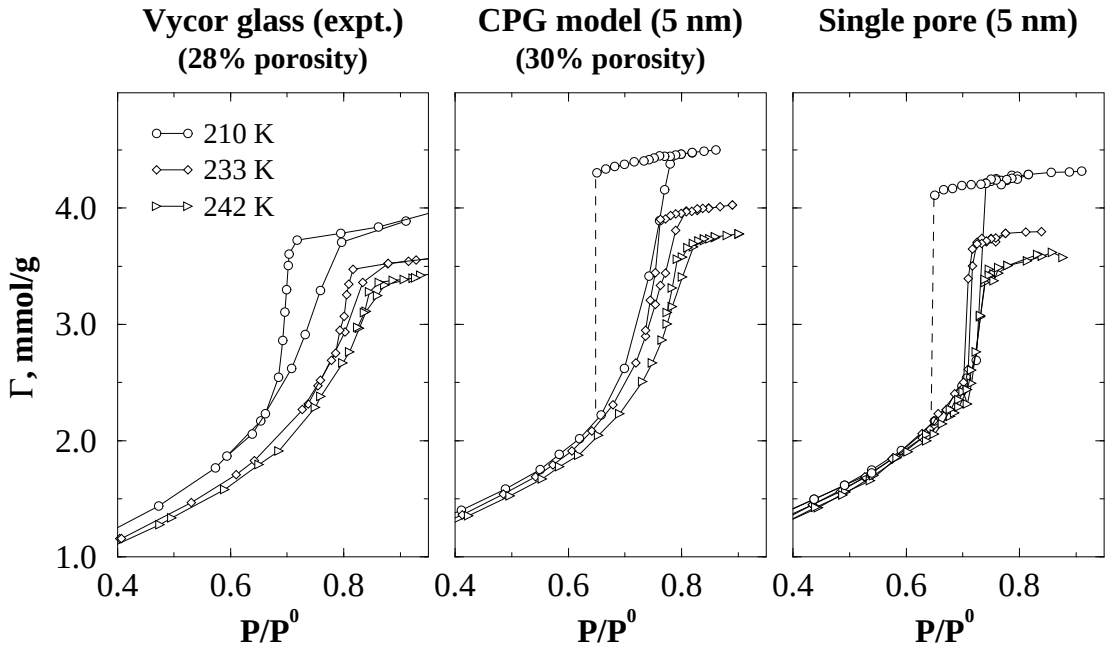

Figure 2. Xenon adsorption in model materials. Experimental data for xenon adsorption on Vycor glass [14] is shown at left, simulated isotherms in the center, and, for comparison, simulations in a single 5 nm cylindrical pore (molecular wall) at right. The adsorption axes all have the same scale. The shape of the experimental adsorption isotherm (and desorption isotherm, at the higher temperatures) is reasonably reproduced by the new models, a substantial improvement over the single-pore approach.

where the pores were filled with liquid were generally equilibrated for 200 million moves, followed by another 200 million moves for data collection; points on the capillary upswing of the adsorption branch and the shoulder of the desorption branch took as many as 2.4 *billion* moves for equilibration before a stable value of the density was reached.

For comparison with experimental data, a series of simulated isotherms in the model glass are shown in *Figure 2*. While quantitative agreement has clearly not been achieved, *no* fitting of either the pore model or the fluid model has been used, and, based on previous experience, we expect that better agreement could be obtained by tuning the model properties and fluid parameters. Although the phase separation process that gives rise to the networked structures of these materials is thought to be insensitive to the precise details of the fluids used [15–17], the simplified fluid mixture used here does not have enough *chemical* detail to describe well the actual surface structure of real glasses. These models are therefore most suited for work at higher pressures and for examining capillary condensation phenomena.

4. Pore Connectivity and Phase Transitions

One principal focus of recent theoretical and experimental research in capillary phenomena has been the *nature* of adsorption/desorption phase transitions in porous materials. Most early work supposed that this transition is first-order, in analogy with the bulk liquid-vapor transition. However, with the advent of modern theories of critical phenomena and phase transitions based on scaling laws and the renormalization group the situation has become much less clear [4, 18]. In the discussion that follows, we use "critical" in this strict sense; use of the phrase "capillary critical point" to mean the temperature at which hysteresis disappears (or similar meanings) is avoided, as the nature of the capillary transition is exactly what is being discussed.

In idealized model pores of two-dimensional geometry ("slit" pores) the capillary transition can be truly first-order, and belongs to the 2D Ising model universality class. In one-dimensional idealized pores (cylindrical geometry) only a remnant of a true phase transition is present, as it is known that systems infinite in only one dimension cannot exhibit first-order transitions or

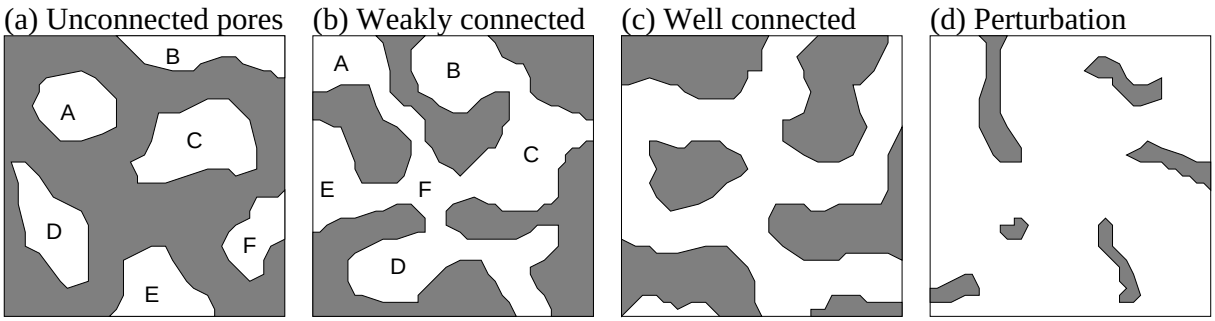

Figure 3. Illustrative sketches of different "coupling regimes" discussed below.

critical points [19, 20]; transitions in cylindrical pores of finite diameter have been discussed elsewhere by ourselves [4, 21–23] and others [24].

Conversely, in extremely high-porosity materials (aerogels) both experimental evidence and theoretical treatments suggest that the presence of the pore material has two major effects; added stabilization of the low-density phase, and interference with density fluctuations at length scales comparable with the material structure [25]. This leads to a shifting of the liquid-vapor phase diagram towards higher densities, and a change in the nature of the critical point from 3D Ising to what looks like a Random-Field Ising Model (RFIM) transition [26, 27]. In the RFIM picture, each "spin" maps onto a relatively large volume of the fluid; since the aerogel is inhomogeneous on length scales less than a few hundred nanometers, its influence on each fluid volume is different, and so the spin is considered to act under a fixed external field of random size and orientation. RFIMs are not as well understood as simple Ising models.

For higher-density materials such as xerogels, controlled pore glasses and Vycor, the picture is more complicated; our discussion applies particularly to materials with relatively small pores, where the effects of confinement are large. We consider the different possible "regimes" of behavior shown in *Figure 3*; the aerogel case discussed above, where the pore network acts as a perturbation at long length scales, is shown at right. The other three cases are pore networks of varying connectivity. In the extreme (and unrealistic) case of independent, *unconnected* pores, the total adsorption isotherm consists of a sum of the adsorption isotherms over a distribution of microscopic pores. Clearly, no critical behavior can occur in such a system, since the correlation length can grow only to the maximum pore dimension and no system-spanning behavior can occur; likewise, the thermodynamic singularities of a true first-order phase transition are not possible [28]. Such a system may still exhibit hysteresis, but as a superposition of hysteresis curves from all the individual pores. Though it is possible in a simulation to use thermodynamic integration to measure the free energies along the adsorption and desorption isotherms and to locate the pressure where these curves cross [29, 30], this point should *not* be interpreted as a global transition pressure.

In the "weakly connected" case (*Figure 3b*), pores are connected by narrowed channels; this is reminiscent of the situation invoked in pore-blocking explanations of desorption hysteresis. This may be a reasonable picture of some experimental materials. In such a system one expects the narrow channels to be filled early in the adsorption process through capillary condensation. If this is the case, it would effectively isolate the different pore sections from each other, since the correlation length in most fluids at conditions not very near the (bulk) critical point is only a few molecular diameters. This would reduce the system to *effectively* unconnected behavior, and again we would expect that, though hysteresis could certainly occur, there is no system-spanning phase transition or real critical behavior.

In *Figure 3c*, the channels connecting the different pore sections have been broadened to the point where it is no longer possible to argue that pore sections would be effectively isolated from each other by capillary condensation in narrow channels. This could be the case in mesoporous materials with quite narrow pore size distributions. If the topological connectivity of the system

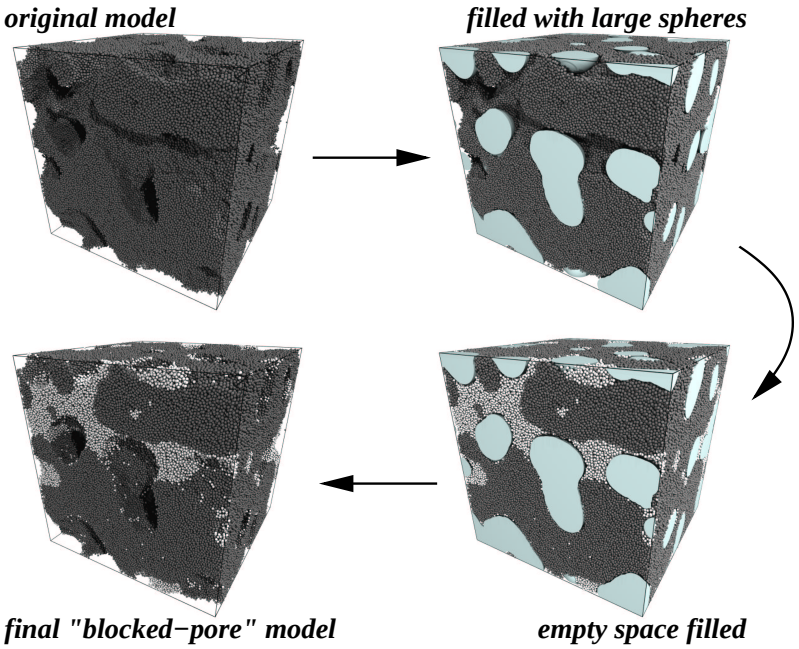

Figure 4. Schematic preparation of blocked-pore models. The original model is filled with overlapping large spheres. The remaining space is then filled with additional pore material (white particles), and upon removal of the large spheres, the pores are recovered, but with fewer connections between them.

is high, "communication" between pore sections could occur even at relatively high loadings, and the possibility of a system-spanning (and therefore first-order) transition appears. The nature (universality class) of the critical point in such a system is difficult to identify; extensive experiments on liquid-liquid equilibria in porous glasses suggest an RFIM-type transition [31–33], with a length scale spanning many pore diameters.

How can molecular simulation be used in resolving this situation? RFIM behavior, if it exists, would occur on a length scale too large (hundreds of nanometers) for any sort of molecular-scale simulation, and the development of coarse-grained, large-length-scale simulation techniques for liquid-vapor equilibria has been slow. Classical Density Functional Theories are, strictly speaking, mean-field theories, and thus prone to predicting phase transitions where there are none, such as in the one-dimensional Ising model [20]. However, molecular simulations ought to be able to provide information that would classify particular systems as either weakly-connected or well-connected; microscopic analysis of simulation data can identify the degree of correlation that exists between different pore sections, and then the arguments just given can be brought to bear.

5. "Blocked-Pore" Models

Our approach to identifying inter-pore correlations in these systems is straightforward. If it is possible to **isolate** (e.g., block off) different pores from each other without changing the adsorption/desorption behavior of the system, then the pores are not "in communication" with each other in the "unblocked" system. If, however, isolation of pores leads to substantial changes in adsorption or desorption, then the connections between pore sections have some active role to play and this can be further investigated. The following procedure, shown schematically in *Figure 4*, is used to prepare "blocked-pore" models, in which inter-pore communication is prevented by additional pore material filling the narrow channels. First, large overlapping spheres are used to "cover" as much of the void space as possible; by choosing the sphere diameter near to the mean pore size, the largest parts of the pore network are covered, and the constrictions remain open. Clearly, the size of the sphere used will influence the degree of coverage. Secondly, the remaining space is filled with additional pore material, effectively blocking off

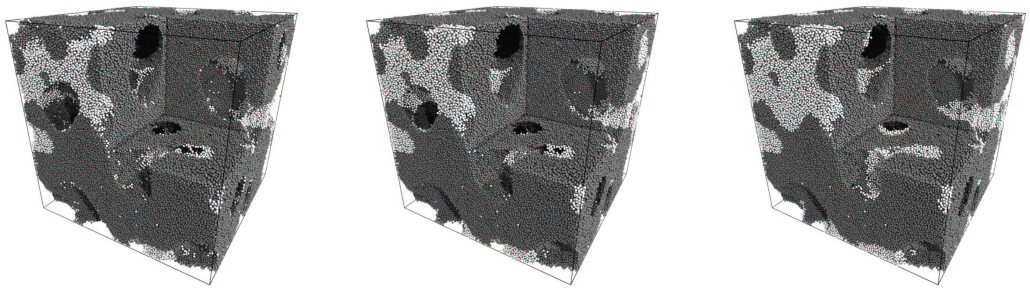

(a) 4.32 nm blocked (b) 4.59 nm blocked (c) 4.86 nm blocked

Figure 5. Blocked-pore models prepared with different size template spheres. The unblocked model is shown in *Figure 1*. As the blocking sphere size increases, more of the pore network is filled, and more of the connections between different parts of the pore network are blocked.

the narrow channels and pore constrictions. Thirdly, the large spheres are removed. The final "blocked-pore" material has a pore size distribution very similar to the original, a somewhat lower porosity, and a much lower *pore connectivity*.

We have used this procedure to prepare the three blocked-pore models shown in *Figure 5*. Adsorption and desorption isotherms have been simulated in the blocked and unblocked models at $k_BT = 0.915\varepsilon$, corresponding to 210 K, approximately 10% below the temperature at which hysteresis disappears in this system, which is approximately $k_BT = 1.02\varepsilon$. The bulk critical point of the model fluid occurs at $k_BT = 1.17\varepsilon$ [34]. These isotherms are shown in *Figure 6*.

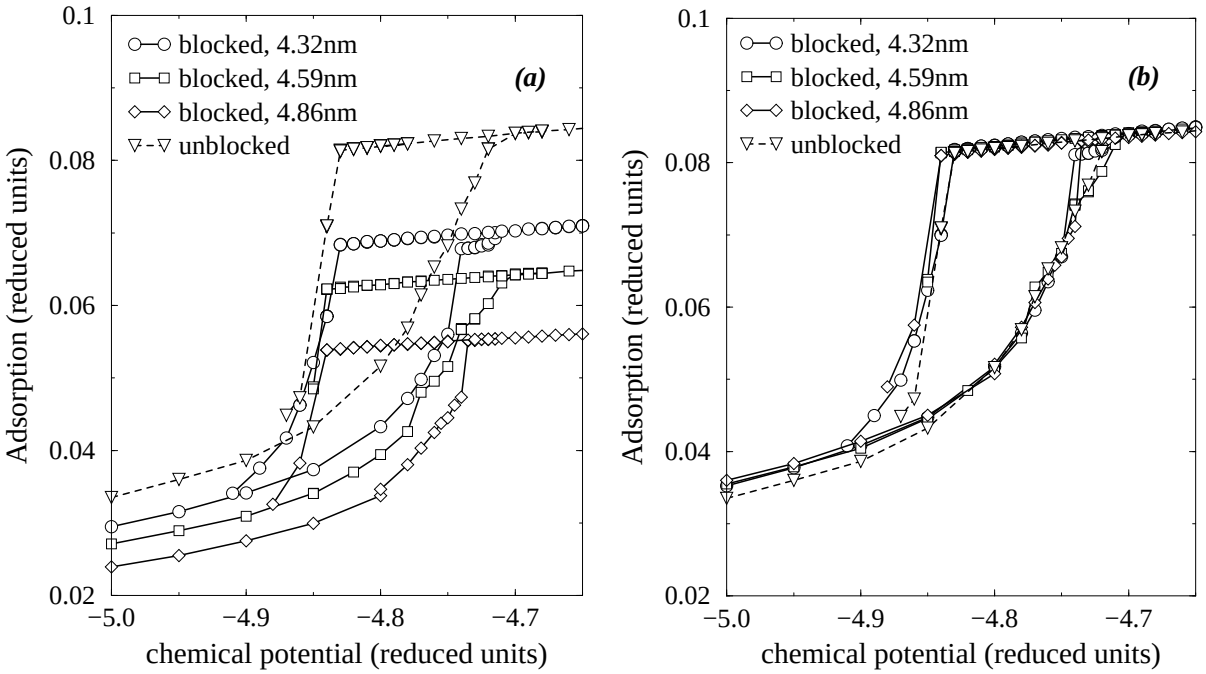

Figure 6. Adsorption and desorption isotherms in the capillary condensation region, for the unblocked model and the three blocked models of *Figure 5*. The isotherms are shown unmodified *(a)* and normalized by porosity *(b)*, for close comparison.

In the unscaled data (left graph) the effect of decreasing porosity in blocked systems is clearly visible, as the maximum adsorption at pore filling is reduced substantially. However, one can correct for this reduction by rescaling the isotherms in the blocked materials to the same total pore volume; this amounts to normalizing the adsorption isotherm by the porosity of the material. Under these conditions it is evident that in the capillary condensation region these materials show essentially identical behavior, since all of these curves superimpose. At

low pressure there is some deviation, which results from changes in the surface area of the blocked-pore models.

Completion of the four adsorption-desorption isotherm pairs shown in this figure consumed approximately 30,000 hours of CPU time on the massively parallel IBM SP computer at the FSU School of Computational Science and Information Technology. On a single-processor machine, this calculation would have run for almost four years; calculations at other temperatures and for other material models are under way at this time.

6. Discussion

The excellent superposition of isotherm data (especially the adsorption branch) in *Figure 6* strongly suggests that in these models the connectivity of the pore network has little or no influence on the shape of the adsorption branch of the isotherm, and little influence on the shape of the desorption branch. This suggests that materials of this type, which include Vycor glass, fall into the "weakly connected" category discussed above. If this is the case, then it is expected that the appropriate thermodynamics for these systems is one of a *collection of quasi-independent microscopic systems*. In such a paradigm there is no system-wide capillary filling or emptying, and the construction of a capillary phase diagram and its comparison with the bulk liquid-vapor phase envelope is misguided.

One motivation for studying capillary critical points is the hope that some of the useful properties of bulk supercritical fluids (which are outstanding solvents) can be accessed in porous systems at near-ambient conditions. In addition to the data shown above, we have obtained isotherms for the unblocked system at both higher and lower temperatures, and microscopically analyzed representative configurations over the entire pressure range. Even at temperatures substantially higher than that at which hysteresis disappears the simulations still exhibit well-defined liquid-vapor interfaces, indicating that the properties of the fluid in the pores are governed by its position on the *bulk* phase diagram. Nothing reminiscent of a "critical fluid" (low density, long-wavelength fluctuations, slow equilibration, etc.) has been observed to date.

These results are consistent with the recent experimental work by Machin [2] who concluded, based on extensive studies of hysteresis loops, that the capillary critical point is not analogous to a bulk critical point. Instead, it is the point where homogeneous nucleation of the vapor phase *replaces* Kelvin-type "failure" of the liquid-vapor meniscus, rather than any sort of phase transition. Our conclusions are also consistent with recent simulation work on realistic Vycor models with smaller pores [35] and in models of other topology [36, 37].

As mentioned briefly above, both the porosity and the pore size distribution are important in determining the character of the pore network. For wide pore size distributions, the probability that condensation in constrictions will lead to isolated-pore behavior is much greater. At fixed pore size, increasing the porosity of a material must result in greater topological connectivity, and thus greater probability of system-spanning behavior. The materials that we have considered to date have only 30% porosity; more porous materials such as xerogels and high-porosity CPG may show true phase transitions.

Acknowledgment. This work was supported in part by a grant from the National Science Foundation (grant no. CTS-9908535).

References

[1] C. G. V. Burgess, D. H. Everett, S. Nuttall, Adsorption of CO_2 and xenon by porous glass over a wide range of temperature and pressure: Applicability of the Langmuir case VI equation, Langmuir (1990), 6, 1734–1738.

[2] W. D. Machin, Properties of three capillary fluids in the critical region, Langmuir (1999), 15, 169–173.

[3] M. Thommes, G. H. Findenegg, Pore condensation and critical-point shift of a fluid in controlled-pore glass, Langmuir (1994), 10, 4270–4277.

[4] L. D. Gelb, K. E. Gubbins, R. Radhakrishnan, M. Sliwinska-Bartkowiak, Phase separation in confined systems, Rep. Prog. Phys (1999), 62, 1573–1659.

[5] W. Haller, Chromatography on glass of controlled pore size, Nature (1965), 206, 693–696.

[6] R. Schnabel, P. Langer, Controlled-pore glass as a stationary phase in chromatography, J. Chromatography (1991), 544, 137–146.

[7] T. H. Elmer, Porous and reconstructed glasses, in: S. J. Schneider, Jr. (ed.), ASM Engineered Materials Handbook, vol. 4, ASM, Materials Park, OH, 1991 427–432.

[8] L. D. Gelb, K. E. Gubbins, Characterization of porous glasses: Simulation models, adsorption isotherms, and the BET analysis method, Langmuir (1998), 14, 2097–2111.

[9] L. D. Gelb, K. E. Gubbins, Pore size distributions in porous glasses: A computer simulation study, Langmuir (1999), 15, 305–308.

[10] M. P. Allen, D. J. Tildesley, Computer Simulation of Liquids, Clarendon Press, Oxford (1987).

[11] A. Brodka, T. W. Zerda, Properties of liquid acetone in silica pores: Molecular Dynamics simulation, J. Chem. Phys. (1996), 104, 6319–6326.

[12] G. S. Heffelfinger, M. E. Lewitt, A comparison between two massively parallel algorithms for Monte Carlo computer simulation: An investigation in the grand canonical ensemble, J. Computat. Chem. (1996), 17, 250–265.

[13] A. Papadopoulou, E. D. Becker, M. Lupkowski, F. van Swol, Molecular dynamics and Monte Carlo simulations in the grand canonical ensemble: Local versus global control, J. Chem. Phys. (1993), 98, 4897–4908.

[14] S. Nuttall, Adsorption and capillary condensation of xenon in porous glass and porous carbon, Ph.D. thesis, University of Bristol (1974).

[15] J. W. Cahn, Phase separation by spinodal decomposition in isotropic systems, J. Chem. Phys. (1965), 42, 93–99.

[16] W.-J. Ma, A. Maritan, J. R. Banavar, J. Koplik, Dynamics of phase separation in binary fluids, Phys. Rev. A (1992), 45, R5347–R5350.

[17] N. S. Andreev, O. V. Mazurin, Kinetics of phase separation, in: O. V. Mazurin, E. A. Porai-Koshits (eds.), Phase Separation in Glass, North-Holland, Amsterdam, 1984 201–242.

[18] J. M. Yeomans, Statistical Mechanics of Phase Transitions, Clarendon Press, Oxford (1992).

[19] L. D. Landau, E. M. Lifshitz, Statistical Physics, vol. 1, Pergamon Press, Oxford, 3rd edn. (1959), Translated by J. B. Sykes and M. J. Kearsley.

[20] D. Chandler, Introduction to Modern Statistical Mechanics, Oxford University Press, New York (1987).

[21] L. D. Gelb, K. E. Gubbins, Studies of binary liquid mixtures in cylindrical pores: Phase separation, wetting and finite-size effects from Monte Carlo simulations, Physica A (1997), 244, 112–123.

[22] L. D. Gelb, K. E. Gubbins, Liquid-liquid phase separation in cylindrical pores: Quench Molecular Dynamics and Monte Carlo simulations, Phys. Rev. E (1997), 56, 3185–3196.

[23] L. D. Gelb, The ins and outs of capillary condensation in cylindrical pores, Mol. Phys. (2001), submitted.

[24] R. Radhakrishnan, K. E. Gubbins, Quasi-one-dimensional phase transitions in nanopores: Pore-pore correlation effects, Phys. Rev. Lett. (1997), 79, 2847–2850.

[25] J. Yoon, D. Sergatskov, J. Ma, N. Mulders, M. H. W. Chan, Superfluid transition of ^{4}He in ultralight aerogel, Phys. Rev. Lett. (1998), 80, 1461–1464.

[26] F. Brochard, P. G. De Gennes, Phase transitions of binary mixtures in random media, J. Physique Lettres (1983), 44, L785–L791.

[27] M. R. Swift, A. Maritan, M. Cieplak, J. R. Banavar, Phase diagrams of random-field Ising systems, J. Phys. A (1994), 27, 1525–1532.

[28] K. Huang, Statistical Mechanics, John Wiley & Sons, New York, 2nd edn. (1963).

[29] B. K. Peterson, K. E. Gubbins, G. S. Heffelfinger, U. Marini Bettolo Marconi, F. van Swol, Lennard-Jones fluids in cylindrical pores: Nonlocal theory and computer simulation, J. Chem. Phys. (1988), 88, 6487–6500.

[30] K. S. Page, P. A. Monson, Phase equilibrium in a molecular model of a fluid confined in a disordered porous material, Phys. Rev. E (1996), 54, R29–R32.

[31] J. V. Maher, W. I. Goldburg, D. W. Pohl, M. Lanz, Critical behavior in gels saturated with binary liquid mixtures, Phys. Rev. Lett. (1984), 53, 60–63.

[32] P. Wiltzius, S. B. Dierker, B. S. Dennis, Wetting and random-field transition of binary liquids in a porous medium, Phys. Rev. Lett. (1989), 62, 804–807.

[33] M. Y. Lin, S. K. Sinha, J. M. Drake, X.-I. Wu, P. Thiyagarajan, H. B. Stanley, Study of phase separation of a binary fluid mixture in confined geometry, Phys. Rev. Lett. (1994), 72, 2207–2210.

[34] N. B. Wilding, Critical-point and coexistence-curve properties of the Lennard-Jones fluid: a finite-size scaling study, Phys. Rev. E (1995), 52, 602–611.

[35] R. J. M. Pellenq, B. Rousseau, P. E. Levitz, A grand canonical monte carlo study of argon adsorption/condensation in mesoporous silica glasses, Phys. Chem. Chem. Phys. (2001), 3, 1207–1212.

[36] L. Sarkisov, P. A. Monson, Computer simulations of phase equilibrium for a fluid confined in a disordered porous structure, Phys. Rev. E (2000), 61, 7231–7234.

[37] E. Kierlik, P. A. Monson, M. L. Rosinberg, L. Sarkisov, G. Tarjus, Capillary condensation in disordered porous materials: Hysteresis versus equilibrium behavior, Phys. Rev. Letts. (2001).